In Silico studies on Triazole derivatives as corrosion inhibitors on mild steel in acidic media.

Ramzi T.T. Jalgham[1]*, Gourisankar Roymahapatra[2], Mrinal Kanti Dash [2]

O. Dagdag[3], Lei Guo[4]

[1]*Department of Oil and Gas, Faculty of Engineering, Bani Waleed University (BWU), Bani Walid, Libya (P.O Box 39221)*

[2] *School of Applied Sciences, Haldia Institute of Technology, Haldia 721657, WB, India*

[3] *Centre for Material Science, College of Science, Engineering and Technology, University of South Africa, Johannesburg 1710, South Africa*

[4]*School of Materials and Chemical Engineering, Tongren University, Tongren 554300, China*

**Corresponding author: ramzittj@bwu.edu.ly*

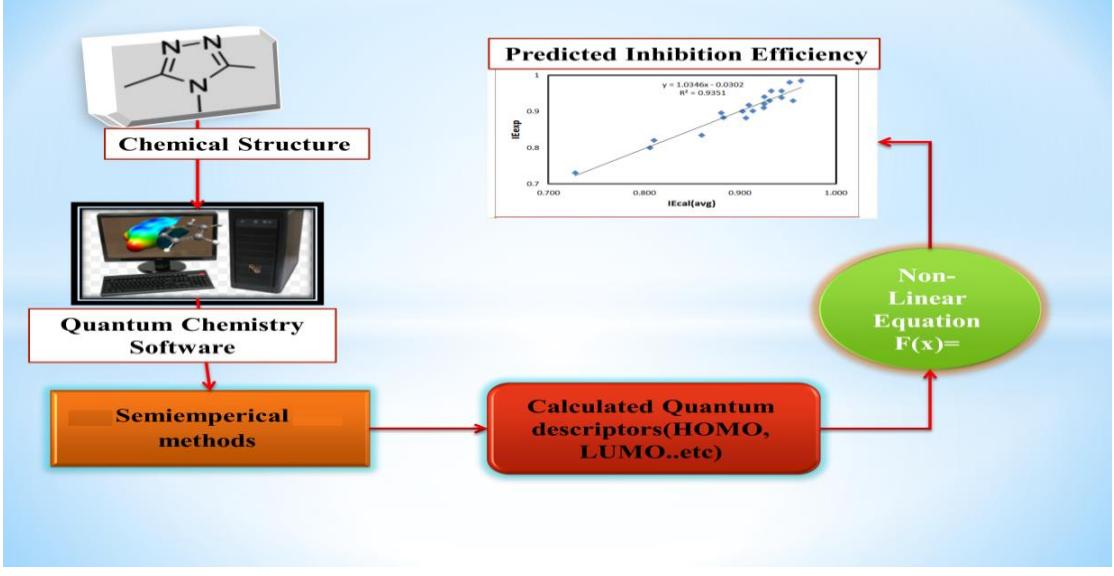

Graphical abstract

Abstract

Theoretical approaches for example quantum calculation and Monte Carlo (MC) simulations are very much important in studying corrosion inhibitors due to a comparatively rapid method of learning the structures. In this article, several semi-empirical quantum calculations methods (AM1, PM3, and PM6) were utilized to study the corrosion inhibition efficiency (*CIE*) of some triazoles as inhibitors of metal corrosion (mild steel introduced to 1 M hydrochloric acid). MC simulation technique was utilized for this study to calculated adsorption energies. Optimized ground state geometries, energy level of highest occupied molecular orbital (E_{HOMO}), energy level of lowest unoccupied molecular orbital (E_{LUMO}), adsorption energies, and dipole moment (μ) were correlated to *CIE* of triazole derivatives. Three equations were suggested to compute CIE. The good agreement was found between CIE_{exp} and CIE_{calc}. The correlation coefficient (R) between CIE_{exp} and CIE_{calc} lies between the ranges of 0.931 to 0.955. AM1, PM3, and PM6 were found to be effective to measure *CIE*. Regression analysis uses fewer quantum parameters when adsorption energy is included in the nonlinear equation. E_{ads} could be able to cut down on the number of descriptors to create models that are easier to use and shorter.

Keywords: Triazole derivatives, QSAR**,** Molecular modelling, semi-empirical calculations methods, Monte Carlo simulation.

1. Introduction

Pipelines are regarded as important machinery for long-distance fluid and gas transportation. In the oil industry, corrosion happens in pipelines at the same time as the removing of oxide layers (pickling). The necessity of using corrosion inhibitors is required[1] to increase the lifetime of steel made pipelines. Anodization is a chemical process that forms an essential part of the electrochemical treatment of metals surface. Pollutants, such as stains, organic

pollutants, inorganic pollutants, etc., are removed from the metal surfaces as part of the surface treatments. Acid solutions primarily cause scale and rust to form. Hydrochloric acid and sulfuric acid are the two acids that are utilized the most. Organic chemical compounds are utilized to lessen the deterioration of metals in hostile environments[2]. as corrosion inhibitors. The choice of ideal corrosion inhibitors mainly influenced by many factors, such as; acceptable inhibitory effectiveness, inexpensive cost, biodegradability, environmentally benign behavior, and long-term stability, all of which should be characteristics of ideal inhibitors. On the other hand, the triazole derivatives are a different group of nitrogen-containing heterocycles that have gained interest Considering the possible uses as eco-friendly corrosion inhibitors, medicines, and coordination chemistries. The capability of these compounds to firmly adsorb on surfaces and achieve acceptable corrosion inhibition efficacy at low concentrations has been emphasized in a number of papers. Moreover, they are very thermally stable substances that are simple to synthesize, effective at low doses, and inexpensive. Researchers are placing a lot of emphasis on triazoles due to their antifungal, antibacterial, and anti-inflammatory properties; these triazole derivative compounds have drawn the attention of several researchers. Thus, the authors selected 18 triazole inhibitors (10 triazole to model and 8 for the validation test of the models), which resemble each other in some manner.

Several methods, including theoretical and experimental ones, are used to investigate how well organic compounds inhibit corrosion. For instance, the most often employed experimental techniques include electrochemical impedance spectroscopy (EIS), potentiodynamic polarization (PDP), and But these processes consume time and costs. All these problems can be prevented by in silico approach. The structures of corrosion inhibitors explain the chemical reactivity. On the contrary, various studies on quantum chemistry have effectively discovered correlations among the effectiveness of inhibition and quantum factors like the energy of molecular orbitals. The quantitative structure activity relationship (QSAR) is a widely used in regression model in chemical investigations and has attracted considerable interest across a wide range of

chemistry fields. Moreover, QSAR is a procedure used to develop a model that is related to molecular structures. Whereas, molecular Modeling is a computer-based technique for drawing, manipulating structures to forecast properties of compounds. The relevant equations to match the experimental results with quantum chemical parameters E_{HOMO}, E_{LUMO}, charges on reactive center, and μ have been developed in a number of efforts [3-7]. With the number of chemicals growing, it is very hard to provide scientists or businesses with the corrosion data they need if just experimental data is used. QSAR is the primary technique for identifying mathematically significant relationships between molecule structure and inhibitory effectiveness. Predicting inhibition efficiency is the main goal of QSAR modeling in corrosion science. A labor, time, and cost-efficient way to find compounds with desired inhibitory qualities is using QSAR. The ideal QSAR should be connected to a clear methodology and a specified area of applicability. The identification of predictive and reliable models that may be used for the future screening of novel and/or untested compounds depends critically on the validation of QSAR models. Many factors can cause some models to fail; including inaccurate data presented in the dataset, or incorrectly choosing an external test set for external validation (absence of external validation) [8-12].

It is a common practice to predict the reactivity of inhibitor compounds using semi-empirical methodologies. Semi-empirical methods (AM1, PM3, and PM6) are crucial for addressing big molecules in computational chemistry since the complete Hartree-Fock technique without approximations is incredibly expensive. By ignoring the approximation of electronic integrals in DFT, semi-empirical methods are derived [13,14]. This results in the introduction of parameters that must be established by experimental data. These results in computing techniques are around three times quicker than the conventional HF/DFT techniques. An advantage of the semi-empirical methods is that the calculation of the optimized structure is easy, and thus the speed of the calculation is very fast. Therefore, semi-empirical approaches are best suited for a particular set of applications; one of these uses is QSAR [15-19]. So, quantum chemical calculations

using three semi-empirical methods were carried out on ten Triazole derivatives. Figure 1 represents the chemical structure of selected triazole. The nomenclature, chemical composition and molecular weight are tabulated in Table 1. Experimental research has shown that, these chemicals are effective in inhibiting corrosion, with efficiencies ranging from 82 to 96% [20]. The objectives of this research are to evaluate theoretically CIE of triazole derivatives using semi-empirical methods and as well as to establish a QSAR model using the derived descriptors. The correlation between CIE and quantum parameters such as E_{HOMO}, E_{LUMO}, and μ are discussed.

Table 1. Names and physical properties of selected triazole compounds

NO	Full name	nomenclature	molecular formula	Molecular weight	Refer No
1	3-hydroxyphenyl-4-phenyl-5-mercapto-1,2,4,triazole	HPMT	C_{14} H_{11} N_3 O S	269.322	21
2	3,4-diphenyl-5-mercapto-1,2,4-triazole	DPMT	C_{14} H_{11} N_3 S	253.323	21
3	3,5-diamino-1,2,4-triazole	TA	C_2 H_5 N_5	99.097	22
4	3,5-Di(m-tolyl)-4-amino-1,2,4-triazole	ATA	C_{18} H_{17} N_5 O2	335.367	22
5	3,5-diphenyl-4H-1,2,4-triazole	DHT	C_{14} H11 N_3	221.263	23
6	3,5-di(m-tolyl)-4H-1,2,4-triazole	m-DTHT	C_{16} H_{15} N_3	249.317	24
7	3,5-bis(4-pyridyl)-4H-1,2,4-triazole	4-PHT	C_{12} H_9 N_5	223.239	24
8	3-cinnamyl-4-phenyl-5-mercapto-1,2,4,triazole	CPMT	C_{16} H_{13} N_3 S	279.361	25
9	2[5-2-pyridyl.-1,2,4-triazol-3-yl] phenol	PPT	C_{13} H_{10} N_4 O	238.250	26
10	3,5-bis(4-methyltiophenyl)-4H-1,2,4-triazole	4-MTHT	C_{16} H_{15} N_3 S_2	313.437	24

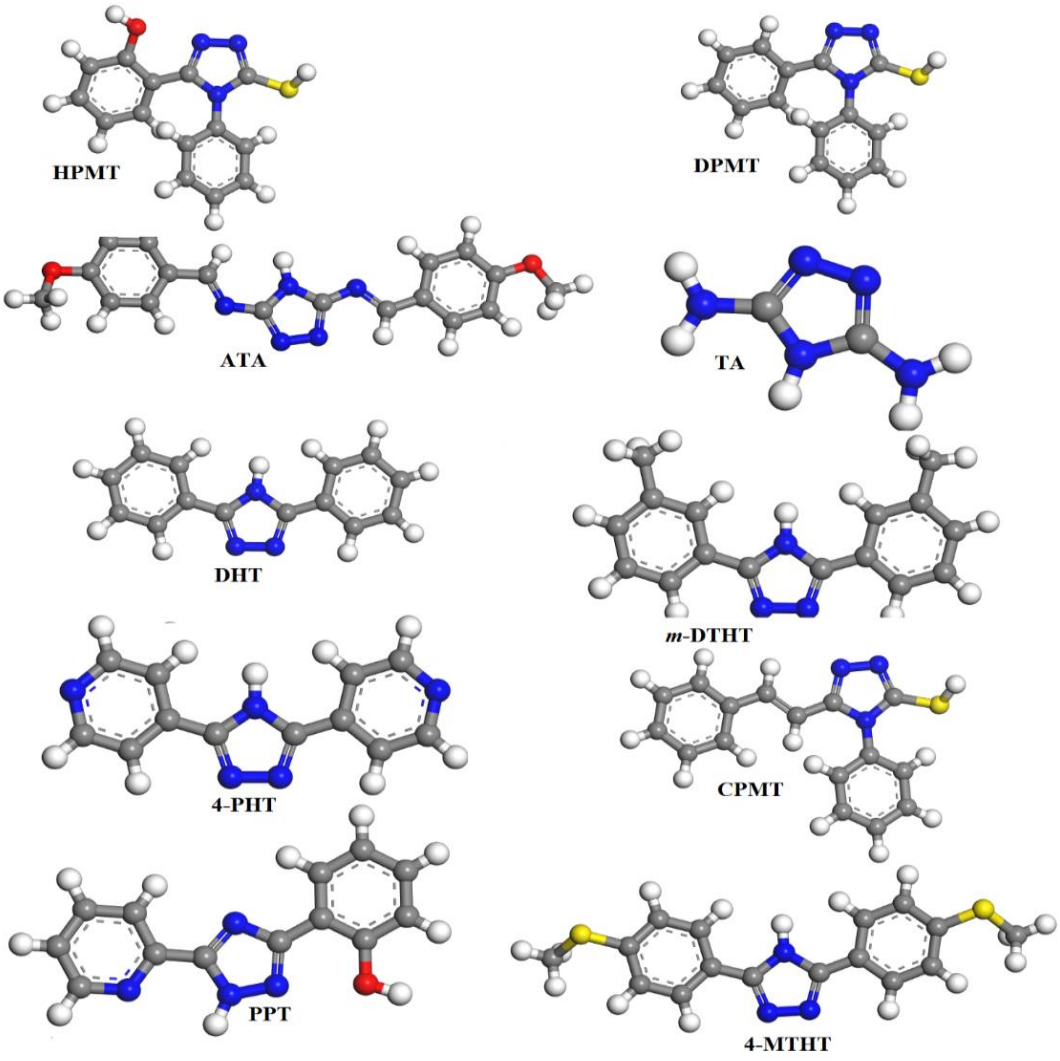

Figure 1. Sketched structures of Triazole derivatives

2. Materials and methods

Using quantum chemical computations, the molecular structures of the chosen substances were examined. The Material Studio 5.5 program for Windows was used to do all of the quantum computations using three semi-empirical approaches at RHF (Restricted Hartree-Fock) level. All inhibitor's structures were fully optimized without any constraints using default program settings [27]. The Bio-Via Materials Studio Interface enables the user to perform the geometry optimization by opening the VAMP dialog. VAMP, a semi-empirical molecular orbital software that has been designed to be very mathematically stable and

quick. Thus, the majority of computations may be performed interactively on personal computers. Most quantum chemistry computations include an essential component called geometry optimization. These techniques are intended to locate the local minimum in their ground state energy surface, where The molecules' frequency ended up to be zero. The obtained optimized structures are similar to substances as they appear in nature. The optimized structures can be used in a variety of studies; theoretical and experimental. The self-consistent field convergence algorithm (SCF) is an iterative procedure and the iterations maximum number was set to 200 with tolerance (10^{-5}). The first step in calculating quantum parameters, Materials Visualizer's sketch tools were employed to sketch molecules. The sketched molecules need to be hydrogenated and cleaned before the Geometry Optimization step. Second step Vamp module was opened, and inside the setup dialog of Vamp module tab, the task was changed to geometry optimization. The calculation methods (Hamiltonian) were changed to AM1, PM3 and PM6 semi-empirical methods, respectively. VAMP reads the Hamiltonian parameters from the Materials Studio website, which regularly updates these parameters (extending the parameterization to additional elements).[28-32] Monte Carlo **(**MC) simulations were employed to calculate adsorption energies of selected inhibitors on Fe_2O_3 (1 1 0) cleaved surface. In this study, the entire Monte MC was conducted by employing the COMPASS as force-field, which is the first superior force-field to investigate properties of large number of organic and inorganic substances. In order to run MC in a simulation cell (29 Å × 23Å × 54 Å) with periodic boundary conditions, the adsorption locator module, COMPASS force field, and the Ewald approach were employed in order to accurately calculate the adsorption energy of selected triazole derivatives. It is essential to check that the settings of structures optimization using the energy minimization parameters should be the same that we want to apply to MC simulation. This covers the accuracy of the computations of geometry optimization energies as well as nonbond summation techniques, the forcefield, and atomic charges. The accuracy of the findings and the computation time are always trade-offs when determining the cut-off. A cut-

off distance (non-bond interactions) of 12.5 Å with a spline switching function was applied for the MC simulation [33].

The SPSS program for Windows, version 10.0, was used to perform statistical analyses. To resolve the non-linear equations, the quantum chemical and adsorption energy parameters (E_{HOMO}, E_{LUMO}, μ and E_{ads}) were taken into account. To do non-linear regression, the Levenberg-Marquardt technique with unconstrained sum of squared residuals in the SPSS software was used. By reducing the sum of the squared differences between the anticipated values (CIE_{calc}) and the experimental values CIE_{exp}, least squares regression calculates the line of best fit (IE_{exp}). Regression is a method for modeling explanatory variables (quantum parameters) and dependent variables (IE_{exp}). A nonlinear equation was entered into the SPSS program along with initial values of regression parameters and a nonlinear regression analysis tool was employed. The least squares technique therefore identifies parameter values that reduce the value of a sum of the squared differences [34].

A correlation coefficient is a measure of the correlation strength or relative movements between two variables. Many different types of correlation coefficient exist, each with its own meaning and its own list of usability and features. Accurate results of R and R^2 will always be in the range between +1 and -1 where the strongest potential model has R and R^2 is extremely near to ±1. When the calculated value of correlation coefficient is greater than 1 or less than -1, it means that there is an error in correlation measurement. The linear relationship's strength and direction are measured by the coefficient of determination (R^2). The Pearson correlation coefficient (R) gauges how closely and effectively two variables are related. (CIE_{exp} and CIE_{calc}). Two essential statistics measurements are R and R^2. Validation is the process of deciding whether the regression results between variables, obtained from regression analysis, are acceptable as descriptions of the data. To evaluate the quality of the model validation tests must be carried out. These coefficients were calculated according to the following equations

$$SS_{Res} = \sum \left(CIE_{exp} - CIE_{calc(avg)}\right)^2 \quad (1)$$

$$SS_{Reg} = \sum \left(CIE_{exp} - CIE_{calc(avg)}(Reg)\right)^2 \quad (2)$$

Where SS_{Res} summation of residuals also known as residual sums and SS_{Reg} the sum of squares; because of the regression or the sum of squares due to the model and CIE (avg) (Reg) were calculated according to following equation.

$$CIE_{calc(avg)}(Reg) = a\ CIE_{calc(avg)} + b \quad (3)$$

a and b are regression parameters between CIE_{exp} and $CIE_{calc(avg)}$

$$R^2 = 1 - \frac{SS_{Reg}}{SS_{Res}} \quad (4)$$

Pearson correlation coefficient

$$R = \frac{(n * \sum CIE_{exp} CIE_{calc(avg)} - \sum CIE_{calc(avg)} \sum CIE_{exp})}{([n \sum CIE_{calc(avg)}{}^2 - (\sum CIE_{calc(avg)})^2])^{0.5} ([n \sum CIE_{exp}{}^2 - (\sum CIE_{exp})^2])^{0.5}} \quad (5)$$

The number of variables in the model is taken into consideration by $R^2_{adjusted}$ (adjusted R-square). Words are only valuable when they enhance the model fit more than would be predicted by chance alone. The adjusted R-squared number falls when the term (E_{ads}) does not sufficiently enhance model.

$$R^2_{adjusted} = 1 - (1 - R^2)\left(\frac{n-1}{n-2}\right) (6)$$

3. Results and discussion

To investigate how well organic compounds inhibit corrosion, it is needed to study the chemical characteristics of existing corrosion inhibitors with both theoretical and experimental techniques and to correlate them to predict structure of projected new analog molecules before their chemical synthesis. This also allows us to select of a accurate inhibitor from a library of chemical molecules. The ideal QSAR should be an unambiguous model and it is easy to handle. A suitable model should include only a few descriptors in order to produce results quickly. E_{ads} may able to reduce the number of descriptors to make models shorter and, it is simple to use. The data of inhibition efficiencies

(CIE_{exp}) of the studied inhibitors was collected from references and these inhibitors were tested (EIS) technique [20]. In this research, three semi-empirical methods were employed in QSAR. The calculated quantum parameters are tabulated in Table 2 by semi-empirical methods for selected compounds.

3.1. Quantum calculations Results

The optimized structures (at the lowest energy, when the change in the molecule's heat of formation approaches to be zero) of Triazole derivatives employing AM1 semi-empirical method are presented in Figure 2. Table 2 presents the values of calculated quantum parameters for triazole derivatives. The HOMO and LUMO energies and how they are distributed among molecules have a crucial role in determining reactivity. The capability of inhibitors to give an electron is typically linked to E_{HOMO}, while E_{LUMO} is associated with the capacity to pull an electron. Higher E_{HOMO} values and lower E_{LUMO} values thus assist the adsorption process [35-37]. Table 1 provides evidence for this, the calculated quantum parameters (E_{HOMO} and E_{LUMO}) of triazole derivatives are not comparable to values of CIE_{exp}. The calculated quantum parameters varied randomly with CIE_{exp}. This data suggests that the inhibitors may not have been either the giver or receiver of electrons. One may infer that there was no electron transport between the active sites of trizole inhibitors and mild steel surface and hence the adsorption may be physical. As shown in Figure 2; (the compounds under study) the HOMO distributions of tiriaozle molecules are primarily localized around the nitrogen, sulphur atoms of the aromatic system [38-42].

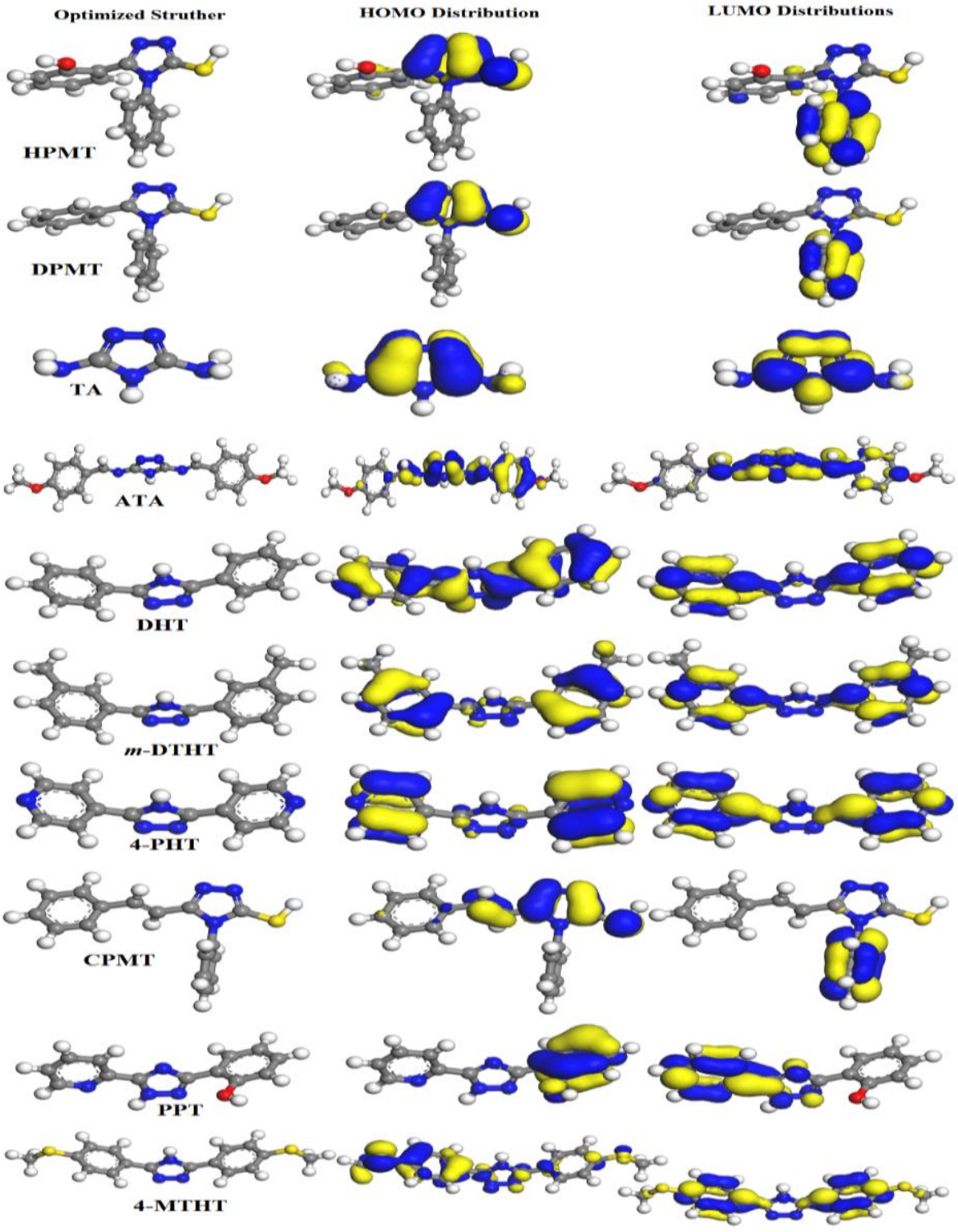

Figure 2. The distribution of HOMO and LUMO of selected Triazole derivatives using AM1 semi empirical method

Table 2. The calculate quantum parameters of selected triazole using semi-empirical methods

Method	Compound	E_{HOMO}(eV)	E_{LUMO}(eV)	μ(Debye)	*Surface area* A^2
AM1	HPMT	-8.035	-0.726	2.536	333.314
	DPMT	-9.348	-1.1345	3.328	234.559
	TA	-8.457	-1.051	2.761	376.278
	ATA	-8.387	-0.776	4.588	297.019
	DHT	-8.676	-0.681	4.614	249.863
	m-DTHT	-8.572	-0.604	4.961	260.934
	4-PHT	-8.579	-0.329	5.43	273.525
	CPMT	-8.840	-0.588	2.098	254.697
	PPT	-9.530	0.312	2.429	116.123
	4-MTHT	-8.713	-0.554	5.664	287.803
PM3	HPMT	-8.432	-1.037	1.987	330.107
	DPMT	-9.465	-1.329	3.643	238.468
	TA	-8.709	-1.110	3.333	374.489
	ATA	-8.641	-1.027	4.907	294.687
	DHT	-8.868	-0.850	4.856	248.588
	m-DTHT	-8.906	-0.696	5.542	271.484
	4-PHT	-8.851	-0.485	5.886	282.437
	CPMT	-9.079	-0.786	1.88	255.046
	PPT	-9.342	0.084	3.909	116.853
	4-MTHT	-8.820	-0.798	5.945	288.471
PM6	HPMT	-8.917	-0.542	4.580	278.331
	DPMT	-8.953	-0.778	4.508	268.920
	TA	-9.495	0.073	3.917	116.724
	ATA	-8.599	-1.083	3.996	372.530
	DHT	-8.991	-0.880	5.613	250.161
	m-DTHT	-9.030	-0.682	7.118	294.949
	4-PHT	-9.824	-1.472	4.118	237.784
	CPMT	-8.797	-0.882	4.450	303.701
	PPT	-8.787	-0.886	1.495	255.555
	4-MTHT	-8.442	-0.871	3.997	336.037

3.2. Monte Carlo simulations

MC simulations were performed on a system that contains Fe_2O_3 surface. The Fe_2O_3 was employed for the MC simulation depends on the iron metal's oxidation prior to the introduction of the acid solution. Table 3 depicts that, 3, 5-Di(m-tolyl)-4-amino-1,2,4-triazole; (ATA) has the highest negative adsorption energy. From Table 3, it can be seen that all the studied inhibitors give adsorption energy in negative values, which suggests that interactions behavior

between triazole derivative and Fe_2O_3 surface oftenly spontaneous adsorption processes and the adsorbed of inhibitors is stable on surface of metal [38-44].

Table 3. The calculated adsorption energy Fe_2O_3 surface .

Compound	HPMT	DPMT	TA	ATA	DHT
E_{ads} (kJ/mol)	-131.473	-128.026	-58.011	-193.696	-127.502
Compound	m-DTHT	4-PHT	CPMT	PPT	4-MTHT
E_{ads} (kJ/mol)	-148.890	-128.115	-153.551	-138.470	-179.359

3.3. QSAR

AM1, PM3, and PM6, QSAR of the 10 compounds (Figure 1) were carried out. From published works, the inhibitors' experimental inhibition efficiency (*CIEexp*) values were gathered. In order to obtain trustworthy productivity assumptions, Quantum parameters and CIE must be well correlated. None of these characteristics, however, have a direct correlation with CIE. Thereby, the Lukovits's non-linear model (NLM). was employed in this research[45]. It is developed from the adsorption isotherm of Langmuir, resulting in the relationship shown below. (1):

$$CIE_{calc} = \frac{(Ax_j + B)C_i}{1 + (Ax_j + B)C_i} \quad (7)$$

Table 4. Regression values outputs.

Method	a	b	c	d	e	f	g
AM1	-11.527	52.775	0.285	18.957	0.016	-1.190	-37.009
PM3	29.516	20.409	0.252	11.018	-0.276	-0.706	393.705
PM6	-1.693	3.167	-5.598	-12.003	-2.539	-0.110	19.841

$$CIE_{calc} = \frac{(-11.527E_{HOMO} + 52.775E_{LUMO} + 0.285\mu + 18.957SA + 0.016E_{ads} - 1.190T - 37.009)C_i}{1 + (-11.527E_{HOMO} + 52.775E_{LUMO} + 0.285\mu + 18.957SA + 0.016E_{ads} - 1.190T - 37.009)C_i} \quad (8)$$

$$CIE_{calc} = \frac{(29.516E_{HOMO} + 20.409E_{LUMO} + 0.252\mu + 11.018SA - 0.276E_{ads} - 0.706T + 393.705)C_i}{1 + (29.516E_{HOMO} + 20.409E_{LUMO} + 0.252\mu + 11.018SA - 0.276E_{ads} - 0.706T + 393.705)C_i} \quad (9)$$

$$CIE_{calc} = \frac{(-1.693E_{HOMO} + 3.167E_{LUMO} - 5.598\mu - 12.003SA - 2.539E_{ads} - 0.110T + 19.841)C_i}{1 + (-1.693E_{HOMO} + 3.167E_{LUMO} - 5.598\mu - 12.003SA - 2.539E_{ads} - 0.110T + 19.841)C_i} \quad (10)$$

Where xj represent a quantum parameters of the inhibitor molecules j; A and B are regression values outputs constants derived by regression analysis; and Ci is the inhibitor concentration. The equations (Eqs) 8 to 10 were generated from Table 4 according to Eq.1. Three equations were suggested to calculate CIE, and their values are listed in Table 5. Each semi-empirical method was employed separately to calculate inhibition efficiency, thus, three values of IE_{calc} are generated. Therefore, the average values ($CIE_{calc(avg)}$) of CIE_{calc} were calculated to avoid of the redundancy of unimportant figures. The correlation between $CIE_{calc(avg)}$ and CIE_{exp} was plotted in Figure 3 from the values in Table 5. An excellent correlation coefficient R^2 has been found between CIE_{exp} and CIE_{calc} where R was ranged from 0.95 to 0.93. The calculated CIE_{calc} and the values of R^2 for each method are listed in Table 5. Figure 4 displays the pattern plots of the average $CIE_{calc(Avg)}$ and CIE_{exp} values for the derivatives of triazoles. In Figure 3, a very high correlation coefficient was observed. This indicates a strong correlation between the experimental and anticipated values. The values of R^2 for each method are reported in Table 5. As can be seen from the highest values of R^2 indicates there is a notable agreement between the outcomes of CIE_{exp} and CIE_{calc}. The evolved models exhibit a strong R^2 according to statistical characteristics, showing that the three proposed models are reliable and predictable [46-50].

Table 5. CIE_{exp} obtained using EIS method of selected trizole and CIE_{calc} obtained by three proposed model.

				CIE_{calc}			
	R			0.951	0.955	0.931	0.962
	R^2			0.905	0.912	0.866	0.926
	Compound	Ci	CIE_{exp}	AM1 Eq.(8)	PM3 Eq.(9)	PM6 Eq.(10)	$CIE_{calc(avg)}$
1	HPMT	9.28×10^{-5}	0.25	0.248	0.254	0.247	0.250
2	DPMT	9.87×10^{-5}	0.542	0.532	0.534	0.620	0.562
3	TA	1.00×10^{-4}	0.58	0.575	0.566	0.587	0.576
4	ATA	1.00×10^{-4}	0.72	0.687	0.686	0.822	0.731
5	DHT	1.00×10^{-4}	0.754	0.830	0.822	0.695	0.782
6	m-DTHT	5.00×10^{-4}	0.798	0.962	0.957	0.856	0.925
7	4-PHT	1.00×10^{-4}	0.853	0.881	0.848	0.871	0.867
8	CPMT	1.07×10^{-3}	0.802	0.818	0.797	0.791	0.802
9	PPT	8.39×10^{-5}	0.937	0.841	0.862	0.858	0.854
10	4-MTHT	5.00×10^{-4}	0.994	0.965	0.948	0.961	0.958

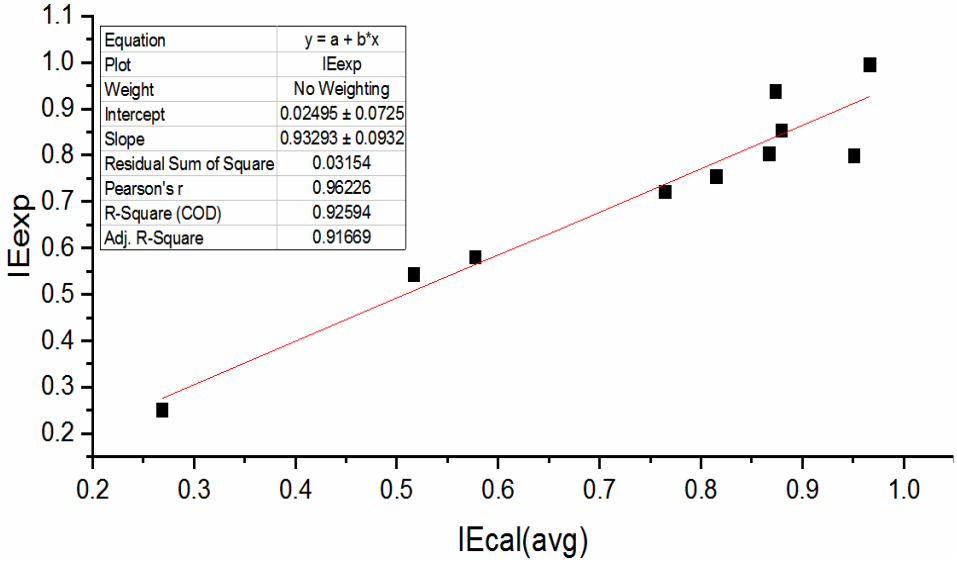

Figure 3. Correlation between CIE_{exp} and $CIE_{calc(avg)}$.

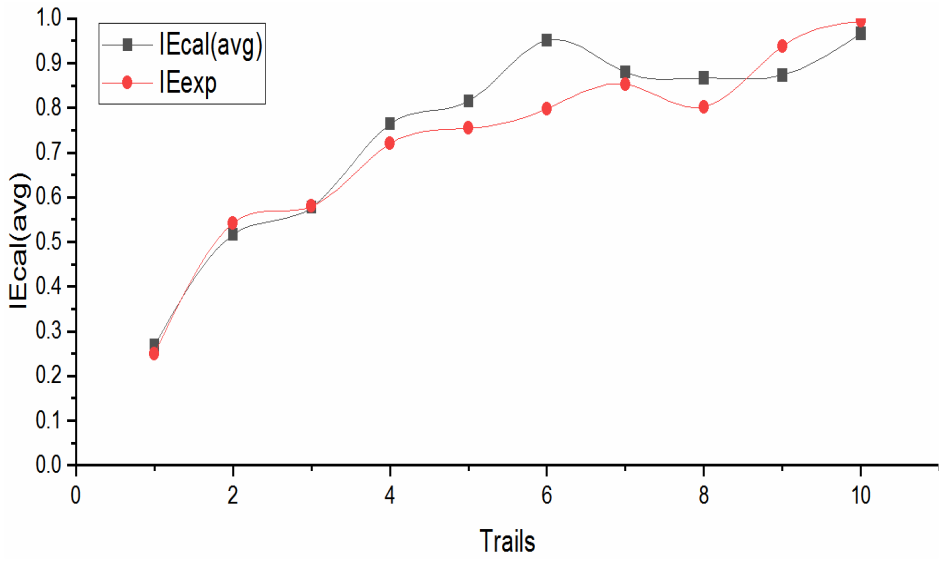

Figure 4. The pattern plot of $CIE_{calc(avg)}$ obtained by equation 8 to 10 and CIE_{exp} at different concentrations of compounds triazole derivatives

The common method used to determine the model stability is to test the effect of this model on sample of different triazole derivatives. The process of checking, whether the models accurately achieve its intended purpose, is called a validation test. The new samples of different triazole derivatives were selected and listed in Table. 6. The basis of the selection of a new set of compounds was that all compounds in the validation test had similar electronic structures to the examined compounds. The quantum calculations and M.C simulations were implemented again with the same previous settings and convergence criteria to calculate E_{HOMO}, E_{LUMO}, μ, E_{ads}. The quantum parameters for the new sample are listed in Table. 6. Next, the Eq. (8) to Eq. (10) (with the same regression constants) were applied on these compounds at different concentrations the estimated values of *CIE* for the new sample of triazoles are tabulated in Table 7. All of these models gave high correlation coefficients fluctuated between 82.25 and 99.63%. The model in fact achieves its intended purpose. It became clear that E_{HOMO}, E_{LUMO}, μ, E_{ads}, parameters have a significant effect on IE of triazole compounds, which is exhibited by the high correlation coefficient from Eq.2, Eq.3 and Eq.4. The possible reason for acquisition better relationships is might

be the addition of E_{ads}. QSAR methodology may be enough to foretell inhibitors efficacy. These relationships might be valuable in planning the design of new inhibitors with appropriate replacements on the heterocyclic compound by joining electron-giving substituents in the organic cycles of triazole compounds. Before the chemical synthesis of new analogs, it is possible to forecast the composition of planned molecules. In this way, designed inhibitor could be chosen from a library of organic compounds. The tree models properly forecast the training data and out-of-sample data but they may not be good or even worthless for prediction of other heterocycle compounds like pyrazoles because of their huge variation in computed quantum parameters.

Table 6. the calculated Quantum parameters of selected triazole compounds using three semi-empirical methods

Method	Compound	E_{HOMO}(eV)	E_{LUMO}(eV)	μ(Debye)	*Surface area* A^2
AM1	3-DTAT	-8.966	-0.414	5.779	306.798
	2-DTAT	-9.251	-0.282	5.379	303.577
	4-DTAT	-8.846	-0.443	5.511	307.408
	APMT	-8.547	-0.432	3.672	278.850
	DBAMTT	-8.496	-0.516	4.39	258.298
	MATD	-9.259	-0.965	7.183	287.893
	SAPMT	-8.595	-0.883	3.739	297.219
	FTA	-8.630	-1.321	6.400	278.139
PM3	3-DTAT	-9.073	-0.661	6.152	304.217
	2-DTAT	-9.605	-0.244	5.571	305.242
	4-DTAT	-8.965	-0.672	5.712	303.718
	APMT	-8.698	-0.544	4.368	287.422
	DBAMTT	-8.425	-1.032	7.988	253.713
	MATD	-9.312	-1.277	8.025	314.676
	SAPMT	-9.052	-0.982	4.924	307.691
	FTA	-8.809	-1.370	6.09	277.014
PM6	3-DTAT	-9.134	-0.588	7.454	307.424
	2-DTAT	-9.459	-0.437	6.790	308.715
	4-DTAT	-8.943	-0.465	6.950	306.839
	APMT	-8.579	-0.641	2.887	281.923
	DBAMTT	-8.448	-0.933	3.146	256.165
	MATD	-9.270	-1.237	9.090	290.177
	SAPMT	-9.071	-1.089	3.703	298.762
	FTA	-9.086	-1.684	6.879	277.037

Table 7. CIE_{exp} and CIE_{calc} of compounds 11–18 (using Eq.(8) to Eq.(10)) estimated using semi-empirical quantum calculation methods.

				CIE_{calc}			
	R			0.806	0.902	0.943	0.925
	R^2			0.650	0.814	0.889	0.856
	Compound	Ci	CIE_{exp}	AM1 Eq.(8)	PM3 Eq.(9)	PM6 Eq.(10)	CIE_{calc}(avg)
11	3-DTAT	5.00×10^{-4}	0.921	0.975	0.947	0.931	0.951
12	2-DTAT	5.00×10^{-4}	0.883	0.976	0.920	0.855	0.917
13	4-DTAT	5.00×10^{-4}	0.957	0.973	0.945	0.949	0.955
14	APMT	9.32×10^{-5}	0.834	0.807	0.801	0.722	0.777
15	DBAMTT	7.00×10^{-4}	0.940	0.974	0.985	0.974	0.977
16	MATD	1.37×10^{-3}	0.938	0.991	0.978	0.991	0.987
17	SAPMT	1.69×10^{-3}	0.956	0.964	0.968	0.995	0.976
18	FTA	3.00×10^{-4}	0.901	0.932	0.926	0.819	0.893

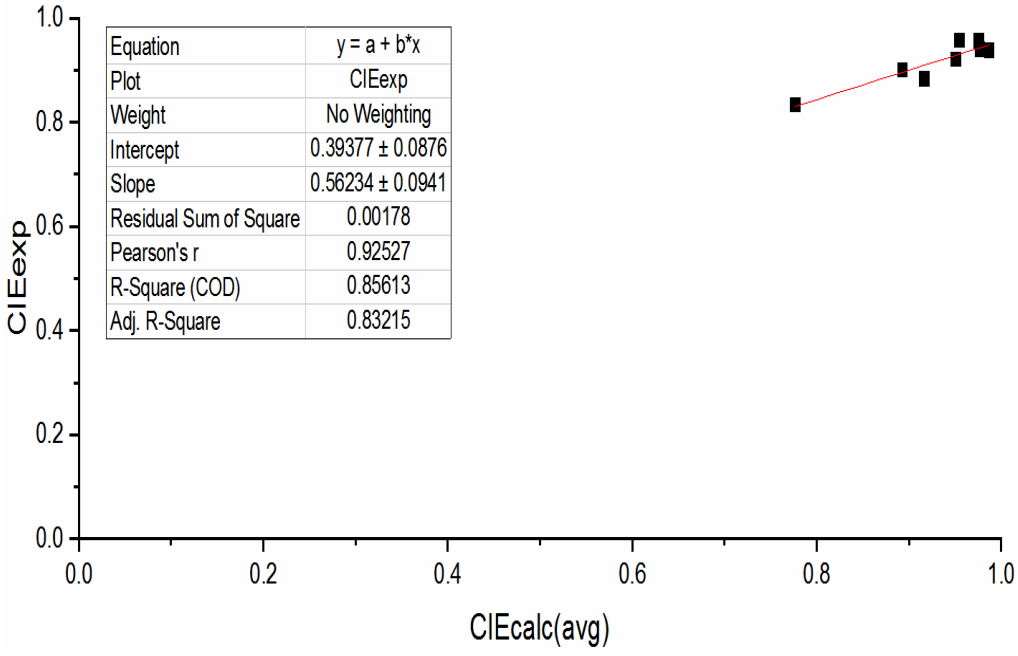

Figure 5. The pattern plots of $CIE_{calc(Avg)}$ and CIE_{exp} for compounds 11-18.

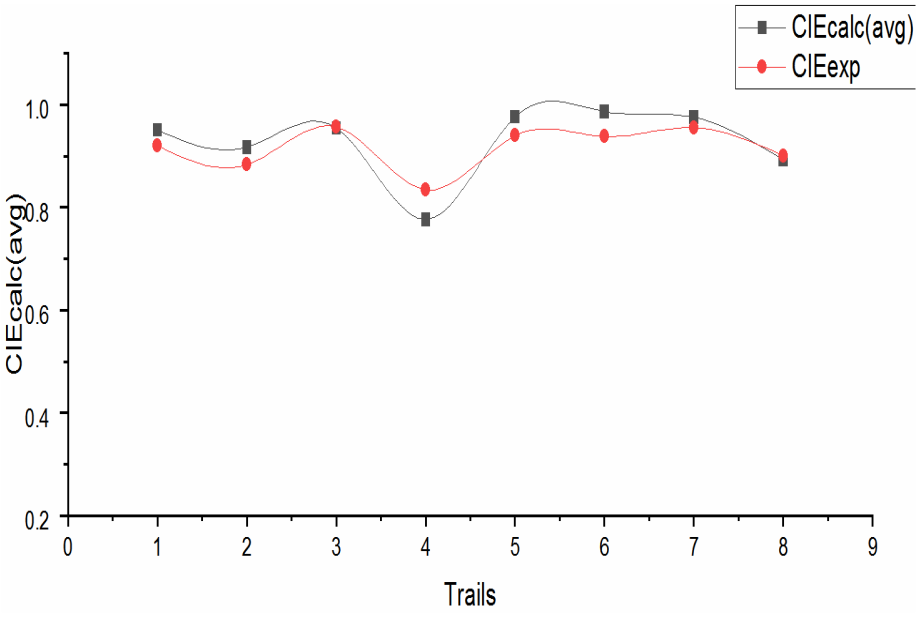

Figure 6. The pattern plot of CIE_{exp} and $CIE_{calc(avg)}$ for compounds 11-18.

5. Conclusions

In this paper; a composite index of many descriptor quantum parameters has been taken into account to describe the corrosion inhibitory performance (*CIE)* of the triazole derivative molecules. The relationships between CIE_{exp} and CIE_{calc} of triazoles compounds in 1 M HCl acid and some quantum descriptors of the triazole compounds were calculated using three semi-empirical methods. The proposed model has a high degree of reliability between theory and experiment, with respect to the statistical review and validation. By linking electron-giving substituents in the organic cycles of triazole compounds, these connections may be helpful in the fabrication of novel inhibitors with proper replacements on heterocyclic compounds. The structure of intended molecules can be predicted before the chemical synthesis of new analogs. This allowed for the selection of a specific inhibitor from a library of chemical molecules. The tree models accurately predict the training data and out-of-sample data, but due to the significant range in calculated quantum parameters for other heterocycle compounds, such as pyrazole, imidazole, oxadiazole, pyrazoline… etc, they may not be good or perhaps useless for this purpose. The statistical methods used in this article can be used to create predictive QSAR models that can forecast the

corrosion inhibitory behavior of organic molecules and to design new corrosion inhibitors in future. We recommended researchers to focus more on these parameters in their research as a result.

Acknowledgements

This article is dedicated to celebrate 162 Birthday of Acharya Prafullya Chandra Ray, the Father of Indian Chemistry. This work was partly sponsored by the National Natural Science Foundation of China (21706195, 22062022) and the Foundation of the Department of Education of Guizhou province (KY[2018]030).

References

1. L. T. Popoola, A. S. Grema, G. K. Latinwo, B. Gutti, A. S. Balogun, Corrosion problems during oil and gas production and its mitigation, *Int J Ind Chem*, 2013, **4**, 35, doi: 10.1186/2228-5547-4-35.
2. J. Fang, J. Li, Quantum chemistry study on the relationship between molecular structure and corrosion inhibition efficiency of amides, *THEOCHEM*, 2002, **593**, 179-185, doi: 10.1016/s0166-1280(02)00316-0.
3. N. K. Allam, Thermodynamic and quantum chemistry characterization of the adsorption of Triazole derivatives during Muntz corrosion in acidic and neutral solutions, *Appl. Surf. Sci*, 2007, **253**, 4570-4577, doi: 10.1016/j.apsusc.2006.10.008.
4. E. El Ashry, A. El Nemr, S. A. Essawy, S. Ragab, orrosion inhibitors Part III: Quantum chemical studies on the efficiencies of some aromatic hydrazides and Schiff bases as corrosion inhibitors of steel in acidic medium, *Arkivoc*, 2006, **11**, 205-220, doi: 10.3998/ark.5550190.0007.b21
5. F. Bentiss, C. Jama, B. Mernari, H. Attari, L. Kadi, M. Lebrini, M. Traisnel, M. Lagrenee, Corrosion control of mild steel using 3,5-bis(4-methoxyphenyl)-4-amino-1,2,4-triazole in normal hydrochloric acid medium, *Corros. Sci*, 2009, **51**, 1628-1635, doi: 10.1016/j.corsci.2009.04.009.
6. O. Dagdag, A. El Harfi, M. El Gouri, Z. Safi, R. T. Jalgham, N. Wazzan, C. Verma, E. Ebenso, U. P. Kumar, Anticorrosive properties of Hexa (3-methoxy propan-1,2-diol) cyclotri-phosphazene compound for carbon steel in 3% NaCl medium:

gravimetric, electrochemical, DFT and Monte Carlo simulation studies, *Heliyon*, 2019, **5**, e01340, doi: 10.1016/j.heliyon.2019.e01340.

7. O. Dagdag, A. Berisha, Z. Safi, O. Hamed, S. Jodeh, C. Verma, E. Ebenso, A. El Harfi, DGEBA-polyaminoamide as effective anti-corrosive material for 15CDV6 steel in NaCl medium: Computational and experimental studies, *J. Appl. Polym. Sci*, 2020, **137**, 48402, doi: 10.1002/app.48402.
8. C. Beltran-Perez, A. A. Serrano, G. Solís-Rosas, A. Martínez-Jiménez, R. Orozco-Cruz, A. Espinoza-Vázquez, A. Miralrio, A General Use QSAR-ARX Model to Predict the Corrosion Inhibition Efficiency of Drugs in Terms of Quantum Mechanical Descriptors and Experimental Comparison for Lidocaine, *Int. J. Mol. Sci.*, 2022, **23**, 5086. doi: 10.3390/ijms23095086.
9. T. W. Quadri, L. O. Olasunkanmi, O. E. Fayemi, E. D. Akpan, H.-S. Lee, H. Lgaz, C. Verma, L. Guo, S. Kaya, E. E. Ebenso, Development of QSAR-based (MLR/ANN) predictive models for effective design of pyridazine corrosion inhibitors, *Mater. Today Commun.*, 2022, **214**, 111753. doi: 10.1016/j.mtcomm.2022.103163
10. H. Zhao, X. Zhang, L. Ji, H. Hu, Q. Li, Quantitative structure–activity relationship model for amino acids as corrosion inhibitors based on the support vector machine and molecular design, *Corros. Sci.*, 2014, **83**, 261-271. doi: 10.1016/j.corsci.2014.02.023.
11. P. B. Raja, M. G. Sethuraman, Natural products as corrosion inhibitor for metals in corrosive media—a review, *Mater. Lett.*, 2008, **62**, 113-116. doi: 10.1016/j.matlet.2007.04.079.
12. R. P. Verma, C. Hansch, Camptothecins: a SAR/QSAR study, *Chem. Rev.*, 2009,**109**, 213-235. doi: 10.1021/cr0780210
13. R. Parida, S. Das, L. J. Karas, I. Judy, C. Wu, G. Roymahapatra, S. Giri, Superalkali ligands as a building block for aromatic trinuclear Cu (I)–NHC complexes, *Inorg. Chem. Front*, 2019, **6**, 3336-3344, doi: 10.1039/C9QI00873J.
14. G. Roymahapatra, S. Giri, D. Sarkar, T. Mondal, A. Mahapatra, W. Hwang, J. Dinda, Synthesis, structure, electrochemistry, fluorescent and DFT study of RuII complexes with pincer-type 2,6-bis (N-methylimidazolylidene/ benzimidazolylidene)- pyrazine ligands, *J. Indian Chem. Soc*, 2015, **92**, 79-88. doi: 10.5281/zenodo.5602987.

15. G. Roymahapatra, S. M Mandal, W. F Porto, T. Samanta, S. Giri, J. Dinda, O. L Franco, P. K Chattaraj, Pyrazine functionalized Ag (I) and Au (I)-NHC complexes are potential antibacterial agents, *Curr Med Chem*, 2012, **19**, 4184-4193, doi: 10.2174/092986712802430090.
16. M. K. Dash, S. D. Chowdhury, R. Chatterjee, S. Maity, G. Roymahapatra, M. Huang, M. Nath, Z. Guo, C omputational investigation on lithium fluoride for efficient hydrogen storage system, *Eng. Sci*, 2022,**18**, 98-104, doi: 10.30919/es8d658.
17. A. Ghosh, G. Roymahapatra, D. Paul, S. M. Mandal, Theoretical analysis of bacterial efflux pumps inhibitors: Strategies in-search of competent molecules and develop next, *Comput. Biol. Chem*, 2020, **87**, 107275, doi: 10.1016/j.compbiolchem.2020.107275.
18. K. Ghosh, N. Bar, G. Roymahapatra, A. B. Biswas, and S. K. Das, Adsorptive removal of toxic malachite green from its aqueous solution by Bambusa vulgaris leaves and its acid-treated form: DFT, MPR and GA modeling, *J. Mol. Liq*, **363** (2022) 119841. doi: 10.1016/j.molliq.2022.119841
19. C. Williams, M. Whitehead, Standard enthalpies of formation in the gas phase and relative stability of tautomers of C-nitro-1, 2, 4-triazole and isomers of N-alkyl-C-nitro-1, 2, 4-triazole: quantum-chemical studies, *THEOCHEM*, **393**, 9-24. doi: 10.1007/s10593-009-0228-4.
20. M. Faisal, A. Saeed, D. Shahzad, N. Abbas, F. A. Larik, P. A. Channar, T. A. Fattah, D. M. Khan, S. A. Shehzadi, General properties and comparison of the corrosion inhibition efficiencies of the triazole derivatives for mild steel, *Corros. Rev*, 2018, **36**, 507-545, doi: 10.1515/corrrev-2018-0006
21. M. Quraishi, R. Sardar, Aromatic triazoles as corrosion inhibitors for mild steel in acidic environments, *Corrosion*, 2002, **58**, doi: 10.5006/1.3277657.
22. D. Gopi, K. Govindaraju, L. Kavitha, Investigation of triazole derived Schiff bases as corrosion inhibitors for mild steel in hydrochloric acid medium, *J. Appl. Electrochem*, 2010, **40**, 1349-1356, doi: 10.1007/s10800-010-0092-z.
23. B. El Mehdi, B. Mernari, M. Traisnel, F. Bentiss, M. Lagrenee, Synthesis and comparative study of the inhibitive effect of some new triazole derivatives towards

corrosion of mild steel in hydrochloric acid solution, *Mater. Chem, Phys,* 2003, **77**, 489-496, doi: 10.1016/S0254-0584(02)00085-8.

24. F. Bentiss, M. Bouanis, B. Mernari, M. Traisnel, H. Vezin, M. Lagrenee, Effect of some ethoxylated fatty acids on the corrosion behaviour of mild steel in sulphuric acid solution, *Appl. Surf. Sci,* 2007, **253**, 3696-3704, doi: 10.1016/j.apsusc.2006.08.001.
25. M. Quraishi, R. Sardar, Effect of Noble Metal Coating on Carbon Steel Corrosion in High-Temperature Wate, *Corrosion,* 2002, **58**, doi: 10.5006/1.3277308.
26. U. Shankar, R. Gogoi, S. K. Sethi, A. Verma, in *Forcefields for Atomistic-Scale Simulations: Materials and Applications*. Springer, 2022, pp. 299-313. doi: 10.1007/978-981-19-3092-8_15.
27. A. J. Rani, A. Thomas, A. Joseph, Inhibition of mild steel corrosion in HCl using aqueous and alcoholic extracts of Crotalaria pallida–a combination of experimental, simulation and theoretical studies, *J. Mol. Liq.,* 2021, **334**, 116515. doi: 10.1016/j.molliq.2021.116515
28. T. Bredow, K. Jug, Theory and range of modern semiempirical molecular orbital methods, *Theor. Chem. Acc.,* 2005, **113**, 1-14. doi: 10.1007/s00214-004-0610-3.
29. S. Sharma, P. Kumar, R. Chandra, *Molecular Dynamics Simulation of Nanocomposites Using BIOVIA Materials Studio, Lammps and Gromacs,* 2019, 329-341. doi: 10.1016/B978-0-12-816954-4.00007-3
30. S. L. Dixon, K. M. Merz Jr, Fast, accurate semiempirical molecular orbital calculations for macromolecules, *J. Chem. Phys.,* 1997, **107**, 879-893. doi: 10.1063/1.474386
31. F. Bentiss, M. Bouanis, B. Mernari, M. Traisnel, M. Lagrenee, Effect of iodide ions on corrosion inhibition of mild steel by 3, 5-bis (4-methylthiophenyl)-4H-1, 2, 4-triazole in sulfuric acid solution, *J. Appl. Electrochem,* 2002, **32**, 671-678, doi: 10.1023/A:1020161332235.
32. H. El Sayed, A. El Nemr, S. A. Essawy, S. Ragab , S, C orrosion inhibitors part V: QSAR of benzimidazole and 2-substituted derivatives as corrosion inhibitors by using the quantum chemical parameters, *Prog. Org. Coat*, 2008, **61**, 11-20, doi: 10.1016/j.porgcoat.2007.08.009

33. W. Li, Q. He, C. Pei, B. Hou, Experimental and theoretical investigation of the adsorption behaviour of new triazole derivatives as inhibitors for mild steel corrosion in acid media, *Electrochim. Acta,* 2007, **52**, 6386-6394, doi: 10.1016/j.electacta.2007.04.077.
34. E. J. Lien, S. Ren, H.-H. Bui, R. Wang, Quantitative structure-activity relationship analysis of phenolic antioxidants, *Free Radical Biol. Med.,* 1999, **26**, 285-294, doi: 10.1016/S0891-5849(98)00190-7.
35. F. Bentiss, M. Traisnel, H. Vezin, M. Lagrenée, Linear resistance model of the inhibition mechanism of steel in HCl by triazole and oxadiazole derivatives: structure–activity correlations, *Corros. Sci,* 2003, **45**, 371-380, doi: 10.1016/s0010-938x(02)00102-6.
36. Q. Deng, N.-N. Ding, X.-L. Wei, L. Cai, X.-P. He, Y.-T. Long, G.-R. Chen, K. Chen, Identification of diverse 1, 2, 3-triazole-connected benzyl glycoside-serine/threonine conjugates as potent corrosion inhibitors for mild steel in HCl, *Corros. Sci,* 2012, **64**, 64-73, doi: 10.1016/j.corsci.2012.07.001.
37. O. Dagdag, A. El Harfi, Z. Safi, L. Guo, S. Kaya, C. Verma, E. Ebenso, N. Wazzan, M. Quraishi, A. El Bachiri, Cyclotriphosphazene based dendrimeric epoxy resin as an anti-corrosive material for copper in 3% NaCl: experimental and computational demonstrations, *J. Mol. Liq,* 2020, **308**, 113020, doi: 10.1016/j.molliq.2020.113020.
38. A. Y. Musa, R. T. Jalgham, A. B. Mohamad, Molecular dynamic and quantum chemical calculations for phthalazine derivatives as corrosion inhibitors of mild steel in 1 M HCl, *Corros. Sci,* 2012, **56**, 176-183, doi: 10.1016/j.corsci.2011.12.005.
39. K. Khaled, Experimental and molecular dynamics study on the inhibition performance of some nitrogen containing compounds for iron corrosion, *Mater. Chem. Phys,* 2010, **124**, 760-767, doi: 10.1016/j.matchemphys.2010.07.055.
40. K. Khaled, Electrochemical behavior of nickel in nitric acid and its corrosion inhibition using some thiosemicarbazone derivatives, *Electrochim. Acta,* 2010, **55**, 5375-5383, doi: 10.1016/j.electacta.2010.04.079
41. A. Y. Musa, A. B. Mohamad, A. A. H. Kadhum, M. S. Takriff, W. Ahmoda, Quantum chemical studies on corrosion inhibition for series of thio compounds on

mild steel in hydrochloric acid, *J. Ind. Eng. Chem.,* 2012, **18**, 551-555, doi: 10.1016/j.jiec.2011.11.131.

42. P. Alvarez, J. Garcia-Araya, F. Beltrán, F. Masa, F. Medina, Ozonation of activated carbons: Effect on the adsorption of selected phenolic compounds from aqueous solutions, *J. Colloid Interface Sci.,* 2005, **283**, 503-512, doi: 10.1016/j.jcis.2004.09.014.
43. O. Dagdag, A. Berisha, Z. Safi, S. Dagdag, M. Berrani, S. Jodeh, C. Verma, E. E. Ebenso, N. Wazzan, A. El Harfi, Highly durable macromolecular epoxy resin as anticorrosive coating material for carbon steel in 3% NaCl: Computational supported experimental studies, *J. Appl. Polym. Sci.,* 2020, **137**, 49003, doi: 10.1002/app.49003.
44. N. Asadi, M. Ramezanzadeh, G. Bahlakeh, B. Ramezanzadeh, Utilizing Lemon Balm extract as an effective green corrosion inhibitor for mild steel in 1M HCl solution: A detailed experimental, molecular dynamics, Monte Carlo and quantum mechanics study, *J. Taiwan Inst. Chem. Eng,* 2019, **95**, 252-272, doi: 10.1016/j.jtice.2018.07.011.
45. I. Lukovits, E. Kalman, G. Palinkas, Nonlinear group-contribution models of corrosion inhibition, *Corrosion,* 1995, **51**, 201-205, doi: 10.5006/1.3294362.
46. O. Dagdag, Z. Safi, H. Erramli, N. Wazzan, I. Obot, E. Akpan, C. Verma, E. Ebenso, O. Hamed, A. El Harfi, Anticorrosive property of heterocyclic based epoxy resins on carbon steel corrosion in acidic medium: Electrochemical, surface morphology, DFT and Monte Carlo simulation studies, *J. Mol. Liq.,* 2019, **287**, 110977, doi: 10.1016/j.molliq.2019.110977.
47. J. Cruz, E. Garcia-Ochoa, M. Castro, Experimental and theoretical study of the 3-amino-1, 2, 4-triazole and 2-aminothiazole corrosion inhibitors in carbon steel, *J. Electrochem. Soc*, 2002, **150**, 1945-7111, doi: 10.1149/1.1528197.
48. R. T. Jalgham, Theoretical, Monte Carlo simulations and QSAR studies on some triazole derivatives as corrosion inhibitors for mild steel in 1 M HCl, *ES energy environ.*, 2021, **13**, 37-49, doi: 10.30919/esee8c476.
49. N. Khalil, Quantum chemical approach of corrosion inhibition, *Electrochim. Acta*, 2003, **48**, 2635-2640. doi: 10.1016/S0013-4686(03)00307-4.

50. S. Ouchenane, R. Jalgham, S. Rezgoun, H. Saifi, M. Bououdina, Experimental and theoretical studies of the corrosion inhibition properties of 2 amino, 4–6-dimethylpyrimidine for mild steel in 0.5 M H2SO4, *Chem. Afr.*, 2021, **4**, 621-633. doi: 10.1007/s42250-021-00239-7.